Powder Technology 294 (2016) 449–453

Contents lists available at ScienceDirect

Powder Technology

journal homepage: www.elsevier.com/locate/powtec

Short communication

Large-scale physical modelling of carbon dioxide injection and gas flow in coal matrix

Hongwei Yang [a,b], Jiang Xu [a], Shoujian Peng [a], Wen Nie [a,*], Jiabo Geng [a], Chaolin Zhang [a]

[a] State Key Laboratory of Coal Mine Disaster Dynamics and Control, Chongqing University, Chongqing 400044, China
[b] Institute of Mining Engineering, Yibin University, Yibin, Sichuan 644007, China

ARTICLE INFO

Article history:
Received 14 October 2015
Received in revised form 19 January 2016
Accepted 10 March 2016
Available online 11 March 2016

Keywords:
Carbon dioxide injection
Gas flow
Large-scale physical modelling
Gas pressure
Coal matrix

ABSTRACT

In this paper, CO_2 injection and subsequent gas flow in a coal matrix are modelled by a large-scale physical experiment. CO_2 transport in porous media after gas injection is investigated in terms of three aspects: (1) the spatio-temporal volumetric strain of the coal matrix caused by CO_2 injection; (2) gas pressure changes or redistribution in the coal matrix resulting from the gas flow; and (3) thermal analysis of the coal matrix during the injection process.

1. Introduction

Underground storage of carbon dioxide (CO_2) in a coal matrix is one of the areas of primary interest for the reduction of greenhouse gases in the atmosphere. This gas can usually exist in micro-pores of the coal matrix for geologically significant periods [1,2]. The evolution of gas transport in porous media under geo-stress is mainly investigated by numerical methods [3–7] and small-scale sample tests in the laboratory [8–11]. Small-scale samples usually cannot avoid the error of the seepage field induced by the boundary problem [12] and the stress field error considering Saint-Venant's Principle [13]. In addition, a small-scale sample experiment can only simulate the stresses and deformations of two directions and not three as in real life. It is also difficult to investigate the internal gas pressure and temperature for a small-size specimen. To overcome these problems, a large-scale physical model is regarded as being close to the real environment. In our study, a large-scale multi-field coupling physical model is employed to investigate the gas transport in a coal matrix after injection of CO_2 (Fig. 1). Swelling and shrinkage of coal and the evolution of gas injection, transportation, and adsorption in the coal matrix under the initial geo-stress are the important aspects of geological sequestration of CO_2. The experimental objects include (1) the spatio-temporal volumetric strain of the coal matrix caused by CO_2 injection; (2) gas pressure changes or redistribution in the coal matrix resulting from the gas flow; and (3) thermal analysis of the coal matrix during the injection process.

* Corresponding author.
E-mail address: niewen1026@gmail.com (W. Nie).

2. Experimental procedure

The experimental coal is from the Sanhuiyi Coal Mine, Chongqing, China (Fig. 3). Due to tectonic forces, the area shows an obvious earth stress concentration. Because of severe tectonic stress, the coal seam is not suitable for mining but benefits from acting a CO_2 reservoir. Thus, it typically represents one geological condition for a CO_2 reservoir. The major horizontal stress in the region is perpendicular to the ridgeline, while the minor horizontal stress is nearly parallel to the ridgeline. According to similarity theory, the geometry and earth stress field are designed as shown in Table 1 (the simulation depth is ~1000 m). The production of the specimen includes: sampling → squeezing → screening → shaping (for the ratios see Table 2). The coal matrix is divided into five layers and every layer is pressed for 1 h under a shaping stress of 7.5 MPa. During the shaping stage, all the gas pressure and temperature pressure sensors are installed. The box is sealed using a rubber gasket. In order to avoid the effect of air in coal, the vacuum time is 1.0 h (the initial experimental design considers an individual gas: CO_2. The purpose of the vacuum is to avoid the interference of air. This may affect the results in terms of the initial adsorption of CO_2. But with the increased gas pressure and enhancement of CO_2 adsorption capacity, the impact will decrease). Stresses are loaded gradually at different loading rates (a stress increment of 0.05 kN). In the coal matrix, 29 gas pressure sensors and 11 temperature sensors are installed inside the model. The arrangement of sensors is as shown in Fig. 2. Data collection includes gas pressure (range: 0–4 MPa; standard deviation: ±0.1%), strain (range: 0–100 mm; standard deviation:

http://dx.doi.org/10.1016/j.powtec.2016.03.015
0032-5910/

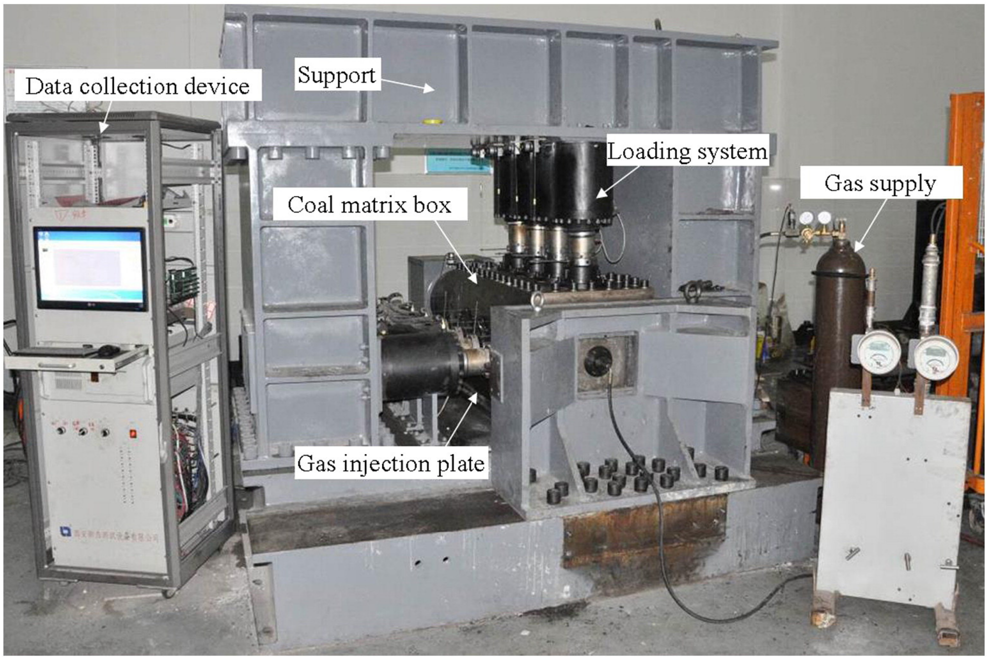

Fig. 1. The physical experiment device.

±0.1%), and temperature (range: −20–100 °C; standard deviation: ±0.1%). The CO_2 is injected uniformly from the plate at the bottom of the box (X = 0). The CO_2 injection pressure is 0.5 MPa.

3. Results

Fig. 4 indicates the changes of gas pressure in three-dimensional directions during the CO_2 injection process. The gap created in the gas pressure (X = 0) after 18 min is due to the change of gas bottle. All the curves represent the average values of sensor readings on each face; for example Z = 133 is the average value of the sensor readings of P24–P28. Fig. 5 describes the volumetric strain in the Z direction during the CO_2 injection process. An increase in strain means there is compressive deformation, while a reduction of strain results from an expansion of the volume. Temperature changes during the CO_2 injection process in the Z direction are shown in Fig. 6.

4. Discussion

In the discussion, we will explore the reasons for the changes in gas pressure and the variations in the volume of the coal matrix and temperature with respect to three stages. Also, the limitations and highlights of the experiment and the direction of future work will be analysed.

Table 1
Stress loading in the X, Y, and Z directions.

Major stress σ_1 (MPa)				Intermediate σ_2 (MPa)	Minor stress σ_3 (MPa)				Gas pressure *P* (MPa)
σ_{14}	σ_{13}	σ_{12}	σ_{11}		σ_{34}	σ_{33}	σ_{32}	σ_{31}	
1.2	1.8	3.0	0.6	1.2	0.72	1.08	1.8	0.36	−0.5

4.1. Gas pressure, volume strain, and temperature of coal matrix

Gas pressure trends are mainly affected by the boundary, earth stress field, adsorption, and coal swelling. Generally, a greater earth stress produces less porosity in the materials, and thus the gas pressure shows higher values in zones of greater earth stress. Also, the position closer to the boundary produces gas aggregation more easily because of the impermeable layer. In Fig. 4(a), Z = 395 and Z = 133 are far away from the effect of earth stress since the sensors are concentrated in the central part (Fig. 2(e) and (d)) (we aim to consider the boundary effects individually). We found that Z = 133 shows higher gas pressure than Z = 395 because the position Z = 133 is close to the face Z = 0. It could be considered that the boundary improves the gas concentration. Z = 657 (Fig. 2(c)) and Z = 919 (Fig. 2(b)) illustrate the effect of both the boundary and the earth stress field. Z = 657 is mainly affected by geo stress (σ_{12} = 3.0 MPa, σ_{32} = 1.8 MPa) and is further away from the face Z = 1050. While Z = 919, which is close to the Z = 1050 (boundary condition) is less affected by geo-stress (σ_{11} = 0.6 MPa, σ_{31} = 0.36 MPa). Z = 919 showed a higher gas pressure, which means the boundary might play a more important role in determining the gas pressure.

In Fig. 4(b), X = 295 is mainly affected by the geo-stress in the face X = 410 (σ_{14}, σ_{13}, σ_{12}, σ_{11}) and is also close to the face X = 410. Thus, it has the highest gas pressure. X = 205 is less affected by the geo-stress in face X = 410 and is further away from both of the faces X = 0 and X = 410. The geo-stress in face X = 410 barely impacts on X = 115, but the boundary X = 0 helps to improve the gas pressure. As a result, the gas pressures at X = 115 and X = 205 are similar. Similarly, in Fig. 4(c), Y = 295 is mainly affected by the geo-stress in the face Y = 410 (σ_{34}, σ_{33}, σ_{32}, σ_{31}) and is also close to the face Y = 410. Thus, it has the highest gas pressure. Y = 205 is less affected by the geo-stress in the face Y = 410 and is further away from both of the faces Y = 0 and

Table 2
Material ratio.

Particle size (mesh)	10–20	20–40	40–60	60–80	80–100	>100	Plaster	Total weight	Moisture
Ratio (%)	35	19	11	5	3	21	6	100	4
Weight (kg)	80.6	43.8	25.3	11.5	6.9	48.4	13.8	240	9.6